Highly efficient and low-cost multispectral photodetector based on RF sputtered a-Si/Ti multilayer structure for Si-photonics applications

F. Djeffal, Nacereddine Boubiche, H. Ferhati, Jacques Faerber, François Le Normand, Nicolas Javahiraly, Thomas Fix

Highly efficient and low-cost broadband multispectral photodetector based on RF sputtered a-Si/Ti structure

F. Djeffal[1,*], N. Boubiche[2], H. Ferhati[1], J. Faerber[3], F. Le Normand[2], N. Javahiraly[2] and T. Fix[2]

[1] LEA, Department of Electronics, University of Batna 2, Batna 05000, Algeria

[2]MaCEPV/ ICube, Université de Strasbourg and CNRS, Strasbourg, France

[3] IPCMS, Université de Strasbourg and CNRS, Strasbourg, France

E-mails: faycal.djeffal@univ-batna2.dz

Tel/Fax: 0021333805494

Abstract

In this paper, a new cost-effective multispectral photodetector (PD) based on amorphous-silicon (a-Si)/titanium (Ti) structure, which achieves a high UV-Visible-NIR photoresponse is elaborated. A new design strategy based on combining FDTD (Finite Difference Time Domain) with GA (Genetic Algorithm) was used to determinate the a-Si/Ti multilayer geometry providing the highest photoresponsivity in UV, Visible and NIR regions. The optimized structure is then fabricated using RF magnetron sputtering technique. A comprehensive analysis of the photodetector electrical, optical and structural properties was carried out. The sputtered a-Si/Ti multilayer was characterized by Scanning Electron Microscopy (SEM), X-ray diffraction (XRD), and UV-Visible-NIR absorption spectroscopy. The a-Si/Ti multilayer PD exhibits a high broadband absorbance of 80% over the UV and even NIR spectrum ranges [200nm-1100nm]. Moreover, photoelectrical characterization showed that the developed device exhibits an improved responsivity under UV, Visible and NIR lights (1.9 A/W at 365nm, 1.24 A/W at 550 nm and 0.93 A/W at 900 nm) and a high I_{ON}/I_{OFF} ratio of 68 dB. The broadband multispectral photodetection property offered by the proposed a-Si/Ti multilayer PD opens a new route for the fabrication of promising alternative photodetectors for future high-performance and cost-effective optoelectronic systems.

Key words: broadband; RF sputtering; multispectral; photodetector; a-Si/Ti.

1. Introduction

Optoelectronic systems based on the Silicon-photonics platform are predicted to be the most practical technology to meet the cost-effective, large bandwidth, and low power consumption requirements [1-4]. Photodetectors (PDs), which are the key components of optoelectronic communication systems, have received an important research interest due to their large applications in biomedical imaging, optical wireless communication, light-detection and robotics [4-8]. Several published works have developed new PD devices, which can detect different wavelength bands ranging from UV to infrared by using adequate semiconductor photosensitive materials with appropriate band-gap values [7-10]. Moreover, the PDs can become more efficient in extensive applications when they are able to detect the broadband multispectral radiations (UV-Visible-NIR) [10-12]. However, the development of multispectral and broadband PDs mainly depends on the control and selection of the suitably matched band-gap materials in order to cover the multispectral range, which is regarded quite challenging. Several works have been proposed to overcome this challenge suggested developing alternative materials and device structures for broadband multispectral photosensing applications. In this context, new design methodologies and structures including plasmonic nanoparticles, core-shell nanostructures, nanowires, metal oxides-based heterojunction and quantum dots have been developed to achieve high broadband absorbance characteristics [10-20]. Despite the capability of these designs to provide the broadband multispectral photodetection, they require costly fabrication techniques and high thermal budget. Additionally, the interface defects associated with different heterostructure materials can affect the carrier transport efficiency and light trapping mechanism, thus limiting the sensor photoresponsivity. In this context, researchers have turned out their focus towards the use of 2D-materials and mono-layers in order to overcome these limitations. This is mainly due to their broadband absorption capability, flexibility and high electron mobility [21-23].

Nevertheless, PDs based on 2D-materials reveal a low responsivity due to severe charge recombination effects and its weak absorption behavior. Therefore, the development of novel efficient and low-cost broadband multispectral photodetectors is required to improve the capabilities of optoelectronic technology. Motivated by this concept, the present work aims at developing a new low-cost and highly efficient multispectral photodetector based on RF sputtered a-Si/Ti multilayer structure for Si-photonic applications. To the best of our knowledge, no design techniques based on experiments assisted by numerical optimization using FDTD and GA computations were conducted to develop broadband multispectral PDs using a-Si/Ti multilayer structure. Accordingly, the optimized a-Si/Ti multilayer structure was prepared using RF magnetron sputtering technique. Structural, optical and electrical characterizations of the elaborated a-Si/Ti-based PD were carried out. It is revealed that the developed PD demonstrates outstanding broadband multispectral absorption capabilities over a wide spectrum range with high electrical performances. Therefore, the proposed approach provides a sound pathway for developing broadband sensors based on simple and low-cost structures for high performance Si-photonics applications.

2. Device design and experiments

The development of Broadband multispectral PDs based on a-Si material is extremely difficult. This constraint is mainly due to the intrinsic limited absorption edge of this material. To overcome this absorption limitation, in this work we investigate a new multispectral PD based on non-hydrogenated a-Si dwells on introducing intermediate Ti ultra-thin layers. In this context, Fig.1 (a) illustrates a cross-sectional view of the investigated a-Si/Ti multilayer-based PD device, where highly transparent ITO thin layer is deposited at the top of the structure to reduce the optical reflection losses [4]. The a-Si/Ti multilayer structure is sputtered considered on a glass substrate. As it is shown in this Figure, $d_{a-Si}=[d_{Si1},d_{Si2},...,d_{Sin}]$ *and* $t_{Ti}=[t_{Ti1},t_{Ti2},...,t_{Tij}]$ represent the thickness victor values

associated with the silicon and titanium layers, respectively. The thickness of the PD device is $t_{a\text{-}Si/Ti}$. For the numerical simulation framework, the optical properties (absorbance, reflectance and transmittance) of the investigated PD structure are calculated using FDTD method provided SILVACO software [24].

As far as we are concerned, the development of highly efficient and low-cost multispectral sensors through intuiting the multi-layer structural, geometrical and electrical parameters by using the well-known optical and electrical properties of PDs is not sufficient to achieve the best electrical performances and highest photoresponsivity over a wide spectrum range. Alternatively, we believe that sophisticated numerical optimization strategies behaving like predictive simulations are required to forecast the sensor performance. In this context, the use metaheuristic optimization approaches such as GA technique is a powerful tool for identifying the optimal geometrical configuration of the a-Si/Ti multilayer structure to achieve the highest multispectral photoresponsivity. To do so, Fig.1 (b) shows the flowchart of the adopted hybrid design approach based on combined GA and numerical simulation techniques. The optical device properties are simulated using 2D-FDTD method. More details regarding the suggested modeling approach can be found in our previously published works [25-27].

The simulated spectral absorbance using FDTD technique is explored to formulate the objective (fitness) function, which will be minimized using GA-based optimization method. The fitness function is given by the following formula

$$Fitness\ (X_i) = \left(\frac{1}{A[\lambda_{\min}, \lambda_{\max}]} \right) \tag{1}$$

where A represents the average absorbance over the spectral range of $[\lambda_{\min}, \lambda_{\max}]$ with $\lambda_{\min} = 200nm$ and $\lambda_{\max} = 1100nm$ are respectively the minimum and the maximum wavelength values considered for broadband photosensing of PDs, X_i denotes the design

parameter vector. Various metals (Ag, Au, Ni and Ti) are introduced in the optimization procedure. After carrying out the optimization procedure, the resulted design parameter victor of the investigated a-Si/Ti multilayer active-film is given by $X_i = (d_{a-Si} = [20nm, 36nm, 50nm, 40nm], t_{ITO} = 20nm, t_{Ti} = [9nm, 8nm, 7nm], j = 3)$. While the optimized metal is the Titanium, the optimized PD structure reveals a very high average absorbance of 83.6% over UV-Vis-NIR spectral range, indicating its broadband sensing properties. This makes it a promising candidate for elaborating highly efficient and low-cost multispectral photodetectors. This enhancement is attributed to the role of GA-based optimization tool in selecting the appropriate multilayer structure through promoting enhanced light-scattering effects. The obtained design will be used to elaborate the optimized a-Si/Ti multilayer sensor, which is the main objective of the next part.

The elaboration of the optimized PD is based on three-step manufacturing processes. In the beginning, glass substrates were ultrasonically cleaned up using an ultrasonic bath and commercial detergent and then dried under a nitrogen jet procedure. Afterwards, successive deposition of the optimized a-Si and Ti thin-films on the glass substrate was carried out using *RF* magnetron sputtering technique (MOORFIELD MiniLab 060). To do so, p-type Si and Ti targets with high purity of 99.99% were used. This experimental technique is commonly used to elaborate high-quality thin-layers [28-30]. The sputtering process was performed in a pure *Ar* atmosphere with a pressure of 1.5 Pa. The deposition parameters were carefully tuned in order to obtain unhydrogenated a-Si state, Besides, the targets to substrate distances were kept at 6.5 cm and 5.1 cm for the Titanium and Si materials, respectively. The sputtering deposition parameters for all sub-layers are summarized in Table.1. The ITO ultrathin film was deposited on the sputtered a-Si/Ti multilayer by using targets with 90 wt% In_2O_3 and 10 wt% SnO_2. It is worthy to note that the RF sputter was calibrated before the deposition of

deferent thin films, where each layer was separately grown on glass substrates to select the appropriate deposition parameters.

In order to assess the optoelectronic performances of the fabricated sensor, structural and optical characterizations were conducted using X-ray diffraction measurements (ARL Equinox 3000) for 2θ diffraction angle scans of [25°-80°] and UV-Visible-NIR spectrophotometer (F10-RT-UV). The morphological characteristics of the prepared sample were analyzed using scanning electron microscopy (SEM), where the surface (top) was imaged with a Zeiss Gemini SEM 500 with a field emission Schottky source. The semiconductor characterization system (Keithley 4200-SCS) was employed to measure the current-voltage characteristics of the prepared device under dark and illumination conditions.

3. Results and discussions

The aim of this work is to investigate the role of introducing a-Si/Ti multilayered structure with optimized geometry in improving the photosensing performances of PDs over a wide spectral range. The structural properties of the prepared sample based on embedded a-Si and *Ti* sputter-deposited thin-films are investigated using XRD technique. In this context, Fig.2 (a) shows XRD measurements for (2θ) diffraction angle scanning from 25° to 80° of the prepared samples based on ITO/a-Si thin-film and a-Si/Ti multilayered structure. The XRD pattern of the elaborated sample with ITO/a-Si shows a low-intensity XRD peak indexed to the (222) crystal plane of the ITO material. It can be also seen from this spectra the presence of a diffraction peak at 28.5° angle, corresponding the (111) facets of silicon. This indicates that the sputtering of thick Si films ($t_{a\text{-}Si}$=130 nm) enables the formation of Si microcrystals. However, it can be noticed from the XRD pattern of the elaborated a-Si/Ti multilayer structure depicted in Fig.2 (a), the amorphous state of the silicon and ITO sputtered layers, where no coherent XRD peaks are matching these materials. The obtained crystalline characteristics can be explained by the ultralow thickness of the deposited silicon sub-layers,

which can prevent reaching the crystallization phase of the Si material. On the other hand, this pattern demonstrates the presence of crystallized Ti metal, manifesting (101)-oriented film at the diffraction angle of 39.5°. This highlights the beginning of the crystallization phase of the deposited Ti inter-layers. Fig.2 (b) shows the SEM top surface image of the fabricated ITO/a-Si/Ti multilayered sample. It can be seen from this micrograph that granulated ITO surface with roughness characteristics is observed. This indicates that the growth is essentially columnar for the embedded a-Si and Ti sub-layers, which further explains the obtained amorphous state of the sputtered silicon thin-films as it is shown in Fig.2 (a). In other words, as the a-Si and Ti thin-films are embedded by RF sputtering technique, the structure roughness significantly increases and when the grain size is superior to the film thickness, the growth becomes columnar particularly for the deposited layers closest to the surface.

One of the most important criteria that active layers of multispectral PDs should satisfy is to offer a broadband absorption property. To assess the absorption capabilities of the prepared sample based on stacked a-Si and Ti sub-layers with optimized geometry, the absorbance spectra of the elaborated samples were extracted and illustrated in Fig.3. It can be observed from this figure that significant changes concerning the optical behavior of the PD active film are achieved by inserting an optimized a-Si/Ti multilayer. It demonstrates highly improved absorption efficiency exceeding 80% over UV-Vis-NIR spectral range as compared to that of a-Si thin-film (28.2%). This yields a high relative enhancement of 183%. In addition, the obtained experimental results are found in a good agreement with the theoretical ones, thus indicating the accuracy of the exploited numerical modeling technique. This achievement is due to the effectiveness of the introduced FDTD-GA hybrid approach in promoting enhanced light trapping capabilities of embedded a-Si and Ti sub-layers with suitable geometry. In other words, the introduction of Ti intermediate metal films within the a-Si layer can generate optical micro-cavities, which leads to extend the optical path in the PD active layer thereby

resulting in a broadband absorption characteristic. Therefore, the fabrication of such an optimized a-Si/Ti multilayered structure as an MSM photodetector can extend the light harvesting capability into the visible and NIR spectral ranges, making it very promising candidate for the development of high-responsivity broadband PDs at low-cost.

To further investigate the multispectral photoresponse of the prepared PD based on stacked a-Si and Ti thin-films, the sample is realized as an MSM photodetector. In this framework, top and bottom gold contacts were evaporated via E-beam evaporation technique as it is shown in Fig.1 (a). The fabricated device was then illuminated by monochromatic light signals with wavelength values of 365 nm, 550 nm and 900 nm using LED lamps. Consequently, the measured I-V characteristics in darkness and under illumination conditions of the prepared sensors based on a-Si and a-Si/Ti multilayer active films are depicted in Fig.4 (a) and (b) respectively. It can be seen from Fig.4 (a) that the a-Si based PD shows a good photoresponse only in the UV range. On the other hand, Fig.4 (b) demonstrates the ability of the prepared PD with embedded a-Si and Ti sub-layers for providing multispectral photodetection capability. The device shows excellent sensing properties with high photocurrent values of 0.68 mA, 0.22 mA and 0.1 mA under UV, visible and NIR lights, respectively at an applied voltage of 3V. Such finding correlates well with the above-outlined broadband absorption characteristic of the optimized structure based on embedded a-Si and Ti thin-films. Basically, the latter structure shows an extended absorption to the visible and NIR regions, which can enables enhancing the carrier generation mechanism. This effect leads to achieve an improved broadband photoresponse. Moreover, the use of stacked a-Si and Ti layers can enlarge the depletion layer in the active layer due to the Schottky nature of the a-Si/Ti contact. This can in turn improve the separation mechanism of the photo-excited e/h pairs, thus reducing recombination losses. It can be also observed from this figure that the proposed PD based on a-Si/Ti multilayer provides a favorable photocurrent at self-powered

condition, where the measured I-V curves are shifted to negative voltages. This phenomenon is attributed to the degraded homogeneity of the deposited sub-layers, where the sputtering of a-Si and Ti layers closest to the surface is principally columnar as it is above-outlined.

To show the capability of the proposed experiment assisted by FDTD-GA hybrid approach in developing broadband PDs based on simple and low-cost structures, Fig.5 depicts the measured spectral responsivity of the elaborated samples based on a-Si thin-film and stacked a-Si and Ti layers. Clearly, the proposed sensor demonstrates a high responsivity over a large spectral band from UV to NIR as compared to the conventional device. The prepared PD with a-Si/Ti multilayered active film exhibits superior responsivity values of 1.9 A/W, 1.24A/W and 93 mA/W under UV, visible and NIR illumination conditions, respectively. This multispectral photoresponse can be attributed to the role of introducing inter-metallic layer in promoting enhanced antireflection capabilities. Besides, the use of an effective approach based on experiment assisted by combined FDTD-PSO design methodology enables enhancing the photogeneration/collection efficiency.

To show the strength of the prepared multispectral PD based on a simple and low-cost embedded a-Si and Ti thin-films as compared to recently developed ones, a comparative performance analysis is carried out. Accordingly, the associated FoM parameters including current ratio (I_{ON}/I_{OFF} ratio), responsivity and detectivity are extracted and summarized in Table.2. This table confirms the ability of the optimized structure for outperforming other perovskite, silicon and nanostructured multispectral PD structures in terms of FoM parameters [31-40]. Although some reported devices demonstrated superior visible photoresponse, they either exhibited a compromised UV sensitivity, stability issues and/or required the use of critical raw materials and processing complexity. Alternatively, the present PD with stacked a-Si and Ti thin-films provides a new strategy for achieving high and broadband photosensing characteristics at low manufacturing cost. These results clearly demonstrate the great potential

of the proposed a-Si/Ti multilayer structure for multispectral photodetection application.

4. Conclusion

In this work, we have developed a new high-photoresponsivity multispectral PD based on ITO/a-Si multilayer structure. The numerical simulation and optimization of the structure using combined FDTD-GA approach offer improved photoresponsivity and broadband absorption capabilities. The optimized design was employed in fabricating multispectral photodetector using RF magnetron sputtering technique. The device structural and optical properties were investigated using XRD and UV-Vis-NIR spectroscopy methods. It was found that excellent UV-Vis-NIR absorbance with over than 80% average value was recorded which can lead to improve the device photoresponsivity. In this context, the elaborated sensor offers ultra-high responsivity values of 1.9 A/W, 1.24A/W and 0.93 A/W under UV, visible and NIR illumination, respectively. This multispectral photodetection property is mainly attributed to the effective light-management provided by the optimized design. Moreover, it is demonstrated that the elaborated PD based on embedded a-Si and Ti sub-layers can operate in self-powered mode, showing a favorable photocurrent of 0.4 µA. The proposed elaboration methodology can contribute in a fascinating breakthrough towards broadband multispectral photodetector devices based on Si-photonics platform.

References

[1] D. A. B. Miller, “Optical interconnects to silicon,” IEEE J. Sel. Top. Quantum Electron., vol. 6, pp. 1312-1317, 2000.

[2] C. Sun, et al “Single-chip microprocessor that communicates directly using light,” Nature, vol. 528, pp. 534-538, 2015.

[3] S. Manipatruni, M. Lipson, and I. A. Young, “Device Scaling Considerations for Nanophotonic CMOS Global Interconnects,” IEEE J. Sel. Top. Quantum Electron., vol. 19, pp. 1077-1086 , 2013.

[4] H. Ferhati, F. Djeffal, A. Saidi, A. Benhaya, A. Bendjerad, “Effects of annealing process on the structural and photodetection properties of new thin-film solar-blind UV sensor based on Si-photonics technology,” Mater. Sci. Semicond. Process., Vol.121, pp. 105331, 2021.

[5] W. Ouyang, F. Teng, J.-H. He, X. Fang, “Enhancing the Photoelectric Performance of Photodetectors Based on Metal Oxide Semiconductors by Charge-Carrier Engineering,” Adv. Funct. Mater., vol. 29, pp.1807672, 2019.

[6] H. Ferhati, F. Djeffal, “A Novel High-Performance Self-Powered Ultraviolet Photodetector: Concept, Analytical Modeling and Analysis,” Superlattices Microstruct., vol. 112, pp.480-492, 2017.

[7] M. Zhang, D. Zhang, and F. Jing, “Hybrid Photodetector Based on ZnO Nanofiber Polymers with High Spectrum Selectivity,” IEEE Photon. Technol. Lett., vol. 28, pp. 1677-1679, 2016.

[8] N. Naderi, M. Moghaddam, “Ultra-sensitive UV sensors based on porous silicon carbide thin films on silicon substrate,” Ceramics International., Vol. 46, pp. 13821-138260, 2020.

[9] C. Li, W. Huang, L. Gao, H. Wang, L. Hu, T. Chen and H. Zhang, “Recent advances in solution-processed photodetectors based on inorganic and hybrid photo-active materials,” Nanoscale, vol.12, pp. 2201-2227, 2020.

[10] K. Benyahia, F. Djeffal, H. Ferhati, A. Bendjerad, A. Benhaya, A. Saidi,“ Self-powered photodetector with improved and broadband multispectral photoresponsivity based on ZnO-ZnS composite,” J. Alloy. Compd., vol. 859, pp.158242, 2021.

[11] H. S. Nalwa, “A review of molybdenum disulfide (MoS_2) based photodetectors: from ultra-broadband, self-powered to flexible devices,” RSC Adv., vol.10, pp. 30529, 2020.

[12] C. Ji, X. Huang, D. Wu, Y. Tian, J. Guo, Z. Zhao, Z. Shi, Y. Tian, J. Jie, and X. Li, "Ultrasensitive self-driven broadband photodetector based on 2D-WS_2/GaAs type-II Zener heterojunction," Nanoscale, vol.12, pp. 4435-4444, 2020.

[13] J. Miao and F. Zhang, "Recent progress on highly sensitive perovskite photodetectors," J. Mater. Chem. C, vol.7, pp. 1741-1791, 2019.

[14] J. Huang, J. Jiang, L. Hu, Y. Zeng, S. Ruan, Z. Ye and Y-J. Zeng, "Self-powered ultraviolet photodetector based on CuGaO/ZnSO heterojunction," J. Mater. Sci.: Mater. Electron., vol.55, pp. 9003-9013, 2020.

[15] X. Xu, J. Chen, S. Cai, Z. Long, Y. Zhang, L. Su, S. He, C. Tang, P. Liu, H. Peng and X. Fang, "A Real-Time Wearable UV-Radiation Monitor based on a High-Performance p-CuZnS/n-TiO_2 Photodetector", Adv. Mater., vol. 25, pp. 1803165, 2018.

[16] M. Patel, P. M. Pataniya, V. Patel, C. K. Sumesh and D. J. Late, "Large area, broadband and highly sensitive photodetector based on ZnO-WS_2/Si heterojunction," Solar energy, vol.206, pp. 974-982, 2020.

[17] H. Ferhati and F. Djeffal, "High-Responsivity MSM Solar-Blind UV Photodetector Based on Annealed ITO/Ag/ITO Structure Using RF Sputtering," IEEE Sens. J., vol. 19, pp. 7942 - 7949, 2019.

[18] S. Bhandari, D. Mondal, S. K. Nataraj and R. G. Balakrishna, "Biomolecule-derived quantum dots for sustainable optoelectronics," Nanoscale Adv., vol.1, 913-936, 2018.

[19] S. Li, Y. Zhang, W. Yang, H. Liuand and X. Fang, "2D Perovskite $Sr_2Nb_3O_{10}$ for High-Performance UV Photodetectors," Adv. Mater., vol.32, pp. 1905443, 2020.

[20] T. T. Nguyen, M. Patel and J. Kim, "Self-powered transparent photodetectors for broadband applications," J. Surf. Interfac., vol.23, pp. 100934, 2021.

[21] B. Wang, Shi P. Zhong, Z. B. Zhang, Z. Q. Zheng, Y. P. Zhang and H. Zhang, "Broadband photodetectors based on 2D group IVA metal chalcogenides semiconductors," Appl. Mater. Today, vol.15, pp. 115-138, 2019.

[22] C-H. Liu, Y-C. Chang, T. B. Norris and Z. Zhong, "Graphene photodetectors with ultra-broadband and high responsivity at room temperature," Nat. Nanotechnol., vol. 9, pp. 273–278, 2014.

[23] J. Yao and G. Yang, "2D material broadband photodetectors," Nanoscale, vol. 12, pp. 454-476, 2020.

[24] Atlas User's manual, SILVACO TCAD, 2012.

[25] F. Srairi, F. Djeffal and H. Ferhati,“ Efficiency increase of hybrid organic/inorganic solar cells with optimized interface grating morphology for improved light trapping,” Optik, vol. 130, pp. 1092-1098, 2017.

[26] H. Ferhati, F. Djeffal, “Role of Optimized Grooves Surface -Textured Front Glass in improving TiO2 Thin Film UV Photodetector Performance,” IEEE Sens. J., vol. 16, pp. 5618- 5624, 2016.

[27] F. Djeffal, H. Ferhati, “A new high-performance phototransistor design based on both surface texturization and graded gate doping engineering,” J. Comput. Electron, vol. 15, pp. 301–310, 2016.

[28] E. Márquez, E. Saugar, J. M. Díaz, C. García-Vázquez, S. M. Fernández-Ruano, E. Blanco, J. J. Ruiz-Pérez and D. A. Minkov, “The influence of Ar pressure on the structure and optical properties of nonhydrogenated a-Si thin films grown by rf magnetron sputtering onto room temperature glass substrates”, J. Non-Cryst Solids, vol. 517, pp. 32-43, 2019.

[29] S. Y. Lee, Y. S. Park, T. Seong, “Optimized ITO/Ag/ITO multilayers as a current spreading layer to enhance the light output of ultraviolet light-emitting diodes,” J. Alloy. Compd., vol.776, pp. 960-964, 2019.

[30] A. Benhaya, F. Djeffal, K. Kacha, H. Ferhati, A. Bendjerad, “Role of ITO ultra-thin layer in improving electrical performance and thermal reliability of Au/ITO/Si/Au structure: An experimental investigation,” Superlattices Microstruct., vol.120, pp. 419-426, 2018.

[31] H. Ahmad, N. Afzal, M. Rafique, A. A. Ahmed, R. Ahmad and Z. Khaliq, “Post-deposition annealed MoO_3 film based high performance MSM UV photodetector fabricated on Si(100),” Ceramics International, vol. 47, pp. 20477-20487, 2020.

[32] D. Wu, J. Guo, J. Du, C. Xia, L. Zeng, Y. Tian, Z. Shi, Y. Tian, K. J. Li, Y. H. Tsang and J. Jie, “Highly Polarization-Sensitive, Broadband, Self-Powered Photodetector Based on Graphene/$PdSe_2$/Germanium Heterojunction,” ACS Nano, vol. 13, pp. 9907−9917, 2019.

[33] Y. Zhang, W. Xu, X. Xu, J. Cai, W. Yang, and X. Fang, “Self-Powered Dual-Color UV–Green Photodetectors Based on SnO_2 Millimeter Wire and Microwires/$CsPbBr_3$ Particle Heterojunctions”, J. Phys. Chem. Lett., vol. 10, pp. 836–841, 2019.

[34] C. L. Hsu, H. Y. Wu, C. C. Fang, and S. P. Chang, “Solution-Processed UV and Visible Photodetectors Based on Y-Doped ZnO Nanowires with TiO_2 Nanosheets and Au Nanoparticles,” ACS Appl. Mater. Interfaces, vol.5, pp. 2087-2095, 2018.

[35] M. Das, S. Sarmah, D. Barman, B. K. Sarma and D. Sarkar, “Distinct band UV–Visible photo sensing property of ZnO-Porous silicon (PS): p-Si hybrid MSM heterostructure,” Mater. Sci. Semicond. Process., vol.118, pp. 105188, 2020.

[36] F. Cao, W. Tian, K. Deng, M. Wang and L. Li, “Self-Powered UV–Vis–NIR Photodetector Based on Conjugated-Polymer/$CsPbBr_3$ Nanowire Array,” Adv. Funct. Mater., vol.29, pp. 1906756, 2019.

[37] H. Ferhati, F. Djeffal and N. Martin, “Highly improved responsivity of self-powered UV–Visible photodetector based on TiO_2/Ag/TiO_2 multilayer deposited by GLAD technique: Effects of oriented columns and nano-sculptured surface,” Appl. Surf. Sci., vol.529, pp. 147069, 2020.

[38] M. S. Mahdi, K. Ibrahim, N. M. Ahmed, A. Hmood, F. I. Mustafa, S. A. Azzez and M. Bououdina, “High performance and low-cost UV–Visible–NIR photodetector based on tin sulphide nanostructures,” J. Alloy. Compd., 735, 2256-2262, 2018.

[39] Z. Zheng, L. Gan, J. Zhang, F. Zhuge and T. Zhai, “An enhanced UV–Vis–NIR and flexible photodetector based on electrospun ZnO nanowire array/PbS quantum dots film heterostructure,” Adv. Sci., vol.4, pp.1600316, 2017.

[40] G. Chatzigiannakis, A. Jaros, R. Leturcq, J. Jungclaus, T. Voss, S. Gardelis and M. Kandyla, “Laser-Microstructured ZnO/p-Si Photodetector with Enhanced and Broadband Responsivity across the Ultraviolet–Visible–Near-Infrared Range,” ACS Appl. Electron. Mater., vol.9, pp. 2819–2828, 2020.

Figures caption:

Fig.1 (a): Device structure with MSM Schottky PD configuration based on the proposed a-Si/ Ti multilayer structure. **(b)** Flowchart of the adopted hybrid design approach based on combined GA and numerical simulation techniques.

Fig.2 (a) X-ray diffraction patterns of the elaborated a-Si/Ti structure with $t_{a\text{-}Si/Ti}$=170nm and t_{ITO}=20nm. **(b)** SEM images of top surface of the elaborated a-Si/Ti multilayer structure using RF magnetron sputtering technique.

Fig.3: Absorbance spectra of the prepared ITO/a-Si and a-Si/Ti multilayer samples with $t_{a\text{-}Si/Ti}$ =170nm and t_{ITO}=20nm.

Fig.4: Measured I-V characteristics under dark and light-exposure conditions in UV, visible and NIR spectrum bands of **(a)** the conventional device with a-Si active layer, **(b)** the prepared PD based on embedded a-Si and Ti sub-layers.

Fig.5: Spectral photoresponsivity of the prepared PD structures based on a-Si thin-film and a-Si/Ti multilayer.

Tables:

Table.1: Deposition parameters of the sputtered ITO/a-Si/Ti multilayer structure.

Table.2: Overall performance comparison between the elaborated PD and several reported multispectral photodetector devices.

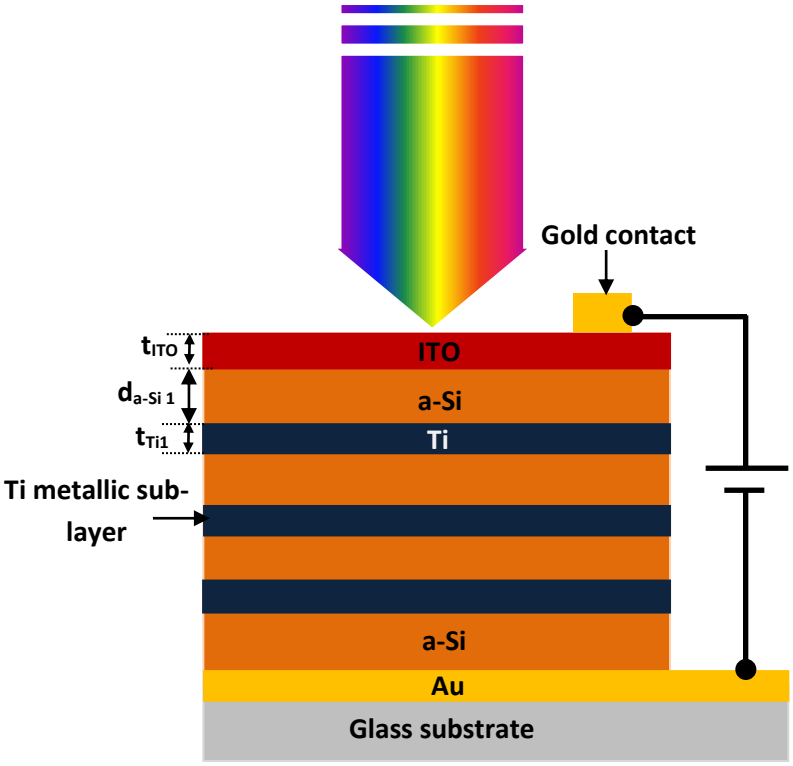
Gold contact
t_{ITO}
ITO
$d_{a\text{-}Si\ 1}$
a-Si
t_{Ti1}
Ti
Ti metallic sub-layer
a-Si
Au
Glass substrate

(a)

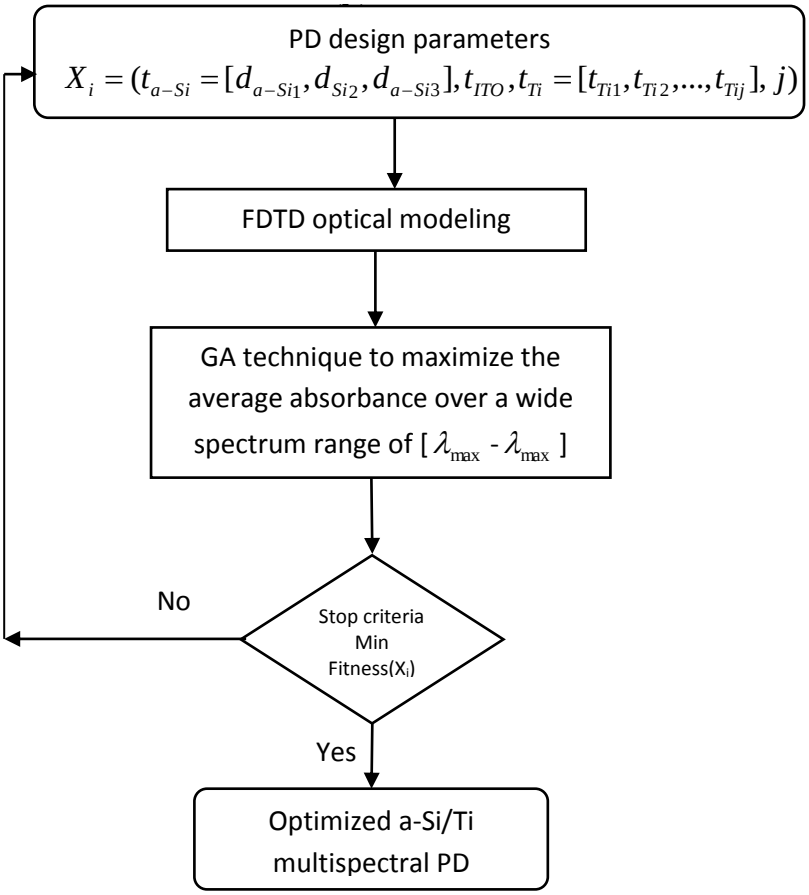
PD design parameters
$X_i = (t_{a-Si} = [d_{a-Si1}, d_{Si2}, d_{a-Si3}], t_{ITO}, t_{Ti} = [t_{Ti1}, t_{Ti2}, ..., t_{Tij}], j)$
FDTD optical modeling
GA technique to maximize the average absorbance over a wide spectrum range of [λ_{max} - λ_{max}]
Stop criteria Min Fitness(X_i)
No
Yes
Optimized a-Si/Ti multispectral PD

(b)

Figure.1

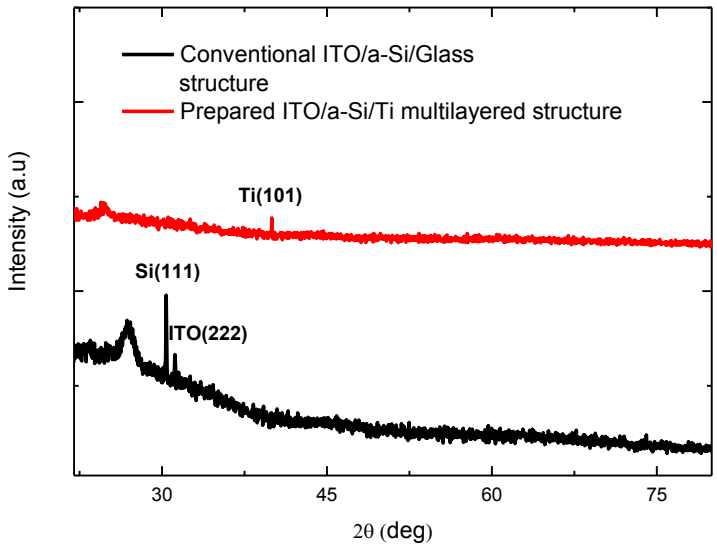
Conventional ITO/a-Si/Glass structure
Prepared ITO/a-Si/Ti multilayered structure
Ti(101)
Si(111)
ITO(222)
Intensity (a.u)
30
45
60
75
2θ (deg)

(a)

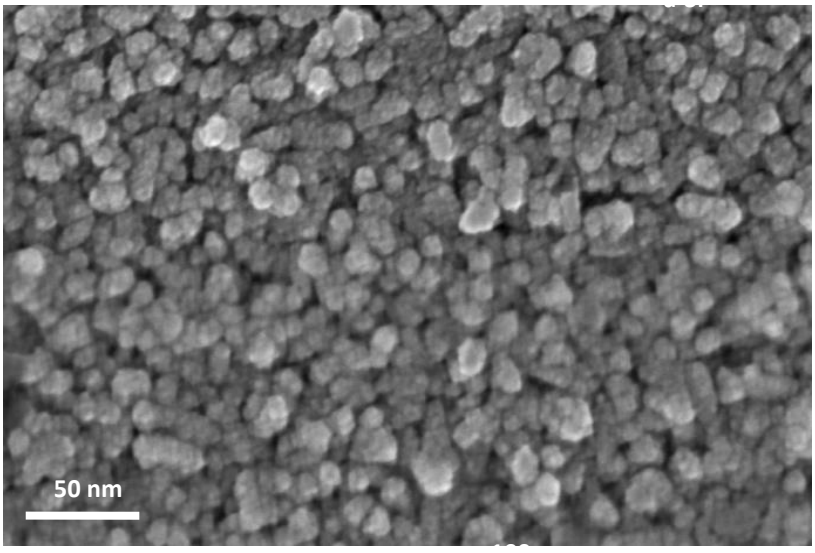
50 nm

(b)

Figure.2

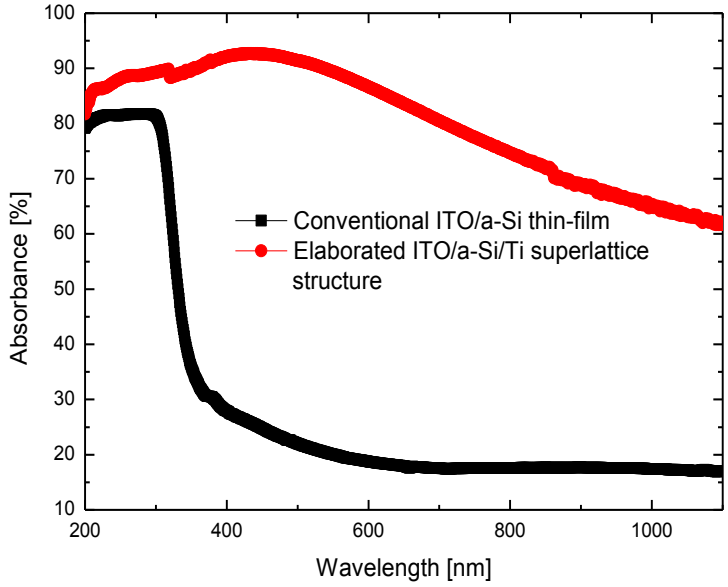
Absorbance [%]
Wavelength [nm]
Conventional ITO/a-Si thin-film
Elaborated ITO/a-Si/Ti superlattice structure
100
90
80
70
60
50
40
30
20
10
200
400
600
800
1000

Figure.3

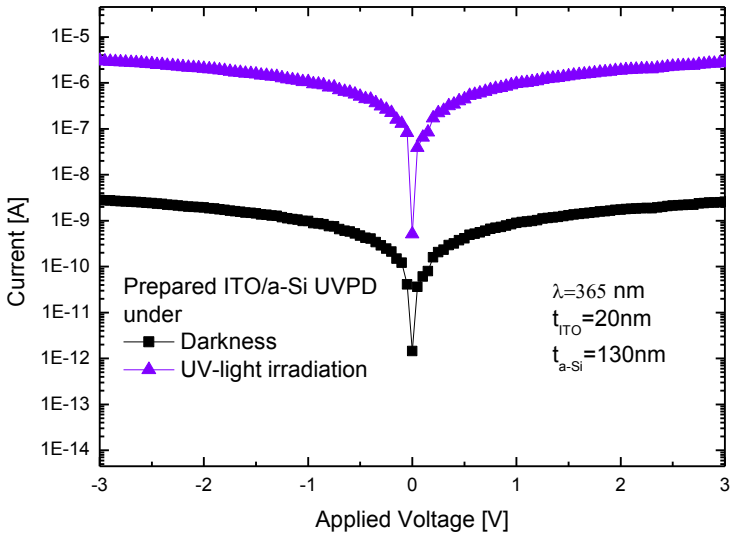
Current [A]
1E-5
1E-6
1E-7
1E-8
1E-9
1E-10
1E-11
1E-12
1E-13
1E-14
-3
-2
-1
0
1
2
3
Applied Voltage [V]
Prepared ITO/a-Si UVPD
under
Darkness
UV-light irradiation
λ=365 nm
t_ITO=20nm
t_a-Si=130nm

(a)

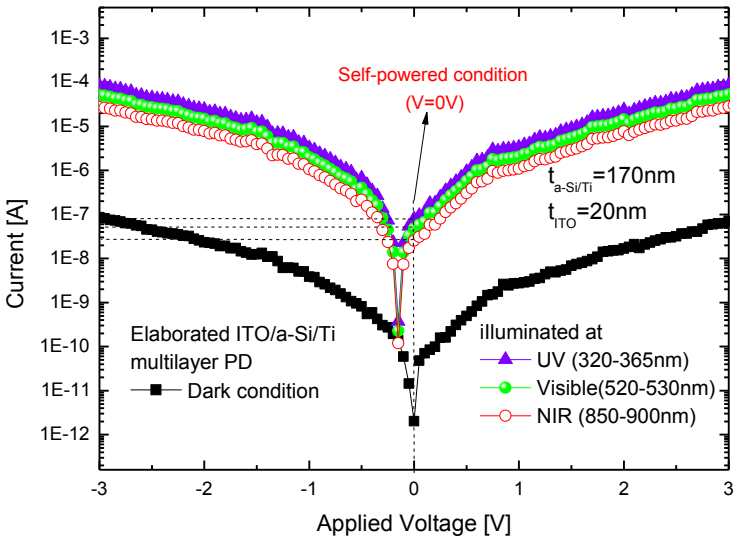
Current [A]
1E-3
1E-4
1E-5
1E-6
1E-7
1E-8
1E-9
1E-10
1E-11
1E-12
-3
-2
-1
0
1
2
3
Applied Voltage [V]
Self-powered condition
(V=0V)
t_a-Si/Ti=170nm
t_ITO=20nm
Elaborated ITO/a-Si/Ti
multilayer PD
Dark condition
illuminated at
UV (320-365nm)
Visible(520-530nm)
NIR (850-900nm)

(b)

Figure.4

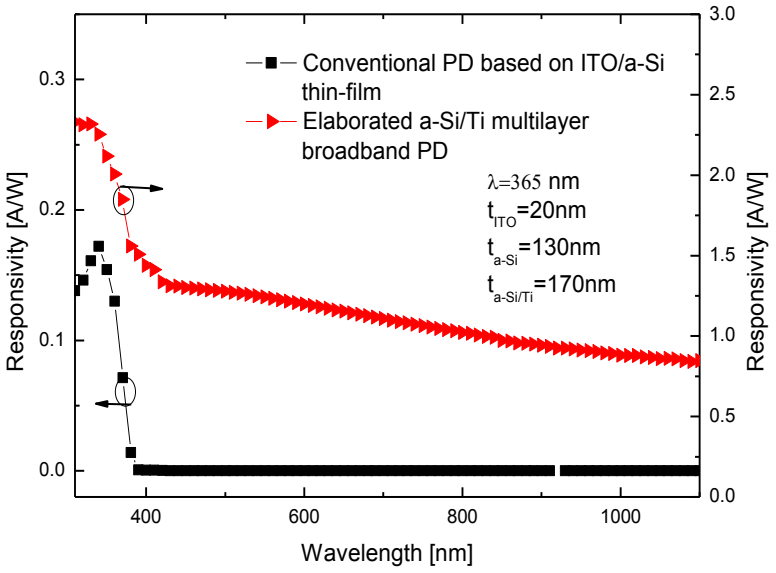
Conventional PD based on ITO/a-Si thin-film
Elaborated a-Si/Ti multilayer broadband PD
λ=365 nm
t_ITO=20nm
t_a-Si=130nm
t_a-Si/Ti=170nm
Responsivity [A/W]
Responsivity [A/W]
Wavelength [nm]
0.0
0.1
0.2
0.3
0.5
1.0
1.5
2.0
2.5
3.0
400
600
800
1000

Figure.5

Table.1

Parameter	**ITO**	**a-Si**	**Ti**
Target	(90% In_2O_3,10% SnO_2)	99.99% p-Si	99.99% Ti
Target to substrate distance (cm)	5	5.1	6.5
Gas composition (Ar: O_2)	(66%: 33%)	/	/
Substrate temperature (K)	300	300	300
power of *RF* source (W)	240	250	250
Working pressure (Pa)	1.5	1.5	1.5
deposition rate (nm/s)	0.2	0.4	0.7

Table.2

UV-Vis-NIR PD structures	UV (320-365 nm)			Visible (green) (515-525 nm)			NIR (880-900 nm)			Ref.
	I_{ON}/I_{OFF} (dB)	R (A/W)	D^* (Jones)	I_{ON}/I_{OFF} (dB)	R (A/W)	D^* (Jones)	I_{ON}/I_{OFF} (dB)	R (A/W)	D^* (Jones)	
MoO_3/c-Si heterojunction	63.2	0.41	3.9×10^{11}	-	-	-	-	-	-	[31]
Graphene/$PdSe_2$/Ge Heterojunction	20	0.69	1.2×10^{13}	28	1.72	2×10^{13}	55.9	4.7	7.4×10^{13}	[32]
SnO_2Microwire/Cs $PbBr_3$ structure	35	0.03	1.6×10^{10}	35.5	0.46	1.2×10^{10}	-	-	-	[33]
Au NPs/p-ZnO NSs/n-ZnO	61.3	0.73	3.4×10^{12}	19.7	0.08	5.3×10^{11}	-	-	-	[34]
ZnO/Si heterjunction	66.2	0.55	4.8×10^{13}	-	0.68	5.8×10^{13}	-	-	-	[35]
Grating $CsPbBr_3/SnO_2$	61.8	0.22	1.2×10^{13}	52.4	0.01	4×10^{12}	53.1	0.086	2×10^{12}	[36]
Inclined TiO_2/Ag/ TiO_2 multilayer	137.2	0.2	5.3×10^{13}	107.6	0.12	3.5×10^{12}	-	-	-	[37]
SnS nanostructure	18	0.38	-	16.8	0.49	-	13.8	0.62	-	[38]
ZnO NWs/PbS QDs	59	0.51	3.4×10^{8}	39	0.07	4.9×10^{7}	26.8	0.11	4.2×10^{7}	[39]
Microstructured ZnO/Si	-	0.6	1×10^{10}	-	0.14	-	-	0.06	-	[40]
a-Si based PD	60.6	0.13	4×10^{12}	/	/	/	/	/	/	This work
a-Si/Ti-based PD	69.1	1.92	9.6×10^{12}	67.2	1.24	6.2×10^{12}	58.5	0.93	4.7×10^{12}	This work

Highlights:

- A new broadband multispectral photodetector based on a-Si/Ti structure is developed.
- Structural, optical and electrical characterizations of the elaborated PD were investigated.
- The proposed multispectral PD exhibits enhanced performances over the conventional sensors.
- The developed photodetector showcases an outstanding performance for Si-photonics technology.

Credit Author Statement

F. Djeffal: Conceptualization, Writing- Reviewing and Editing, Methodology. **N. Boubiche**: elaboration, characterisation. **H. Ferhati:** Writing- Original draft preparation, Software, Validation. **J. Faerber:** characterisation. **F. Le Normand:** characterisation, **N. Javahiraly**: Methodology. **T. Fix:** Methodology

Highly efficient and low-cost multispectral photodetector based on RF sputtered a-Si/Ti multilayer structure for Si-photonics applications

F. Djeffal[1,*], N. Boubiche[2], H. Ferhati[1], J. Faerber[3], F. Le Normand[2], N. Javahiraly[2] and T. Fix[2]
[1] LEA, Department of Electronics, University of Batna 2, Batna 05000, Algeria
[2]MaCEPV/ ICube, Université de Strasbourg and CNRS, Strasbourg, France
[3] IPCMS, Université de Strasbourg and CNRS, Strasbourg, France
E-mails: faycal.djeffal@univ-batna2.dz
Tel/Fax: 0021333805494

Abstract

In this paper, a new cost-effective multispectral photodetector (PD) based on amorphous-silicon (a-Si)/titanium (Ti) multilayer structure, which achieves a high UV-Visible-NIR photoresponse is elaborated. A new design strategy based on combining FDTD (Finite Difference Time Domain) with GA (Genetic Algorithm) was used to determinate the a-Si/Ti multilayer geometry providing the highest photoresponsivity in UV, Visible and NIR regions. The optimized structure is then fabricated using RF magnetron sputtering technique. A comprehensive analysis of the photodetector electrical, optical and structural properties was carried out. The sputtered a-Si/Ti multilayer was characterized by Scanning Electron Microscopy (SEM), X-ray diffraction (XRD), and UV-Visible-NIR absorption spectroscopy. The a-Si/Ti multilayer PD exhibits a high broadband absorbance of 80% over the UV and even NIR spectrum ranges [200nm-1100nm]. Moreover, photoelectrical characterization showed that the developed device exhibits an improved responsivity under UV, Visible and NIR lights (1.9 A/W at 365nm, 1.24 A/W at 550 nm and 0.93 A/W at 900 nm) and a high I_{ON}/I_{OFF} ratio of 68 dB. The broadband multispectral photodetection property offered by the proposed a-Si/Ti multilayer PD opens a new route for the fabrication of promising alternative photodetectors for future high-performance and cost-effective optoelectronic systems.

Key words: broadband; RF sputtering; multispectral; photodetector; a-Si/Ti.

1. Introduction

Optoelectronic systems based on the Silicon-photonics platform are predicted to be the most practical technology to meet the cost-effective, large bandwidth, and low power consumption requirements [1-4]. Photodetector (PD), which is a key component of optoelectronic communication systems, has received an important research interest due to their large applications in biomedical imaging, optical wireless communication, light-detection and robotics [4-8]. Several published works have developed new PD devices, which can detect different wavelength bands ranging from UV to infrared by using adequate semiconductor photosensitive materials with appropriate band-gap values [7-10]. Moreover, the PDs can become more efficient in extensive applications when they are able to detect the broadband multispectral radiations (UV-Visible-NIR) [10-12]. However, the development of multispectral and broadband PDs mainly depends on the control and selection of the suitably matched band-gap materials in order to cover the multispectral range, which is regarded quite challenging. In this context, combining several semiconductor materials to form heterostructure that can cover a wide spectral range leads to induce degradation related to lattice mismatching effects, optical losses and severe recombination effects. These undesired effects prevent the realization of high-performance broadband photodetectors. Several works have been proposed to overcome this challenge suggested developing alternative materials and device structures for broadband multispectral photosensing applications. In this context, new design methodologies and structures including plasmonic nanoparticles, core-shell nanostructures, nanowires, metal oxides-based heterojunction and quantum dots have been developed to achieve high broadband absorbance characteristics [10-20]. Despite the capability of these designs to provide the broadband multispectral photodetection, they require costly fabrication techniques and high thermal budget. Additionally, the interface defects associated with different heterostructure materials can affect the carrier transport

efficiency and light trapping mechanism, thus limiting the sensor photoresponsivity. In this context, researchers have turned out their focus towards the use of 2D-materials and mono-layers in order to overcome these limitations. This is mainly due to their broadband absorption capability, flexibility and high electron mobility [21-23]. Nevertheless, PDs based on 2D-materials reveal a low responsivity due to severe charge recombination effects and its weak absorption behavior. Therefore, the development of novel efficient and low-cost broadband multispectral photodetectors is required to improve the capabilities of optoelectronic technology. Motivated by this concept, the present work aims at developing a new low-cost and highly efficient multispectral photodetector based on RF sputtered a-Si/Ti multilayer structure for Si-photonic applications. To the best of our knowledge, no design techniques based on experiments assisted by numerical optimization using FDTD (Finite Difference Time Domain) and GA (Genetic Algorithm) computations to develop broadband multispectral PDs using a-Si/Ti multilayer structure have been reported. Accordingly, the optimized a-Si/Ti multilayer structure was prepared using RF magnetron sputtering technique. Structural, optical and electrical characterizations of the elaborated a-Si/Ti-based PD were carried out. It is revealed that the developed PD demonstrates outstanding broadband multispectral absorption capabilities over a wide spectrum range with high electrical performances. Moreover, the elaborated photodetector shows high sensitivity values of 1128, 681 and 380 over UV, Visible and NIR spectral bands. Therefore, the proposed approach provides a sound pathway for developing broadband sensors based on simple and low-cost structures for high performance Si-photonics applications.

2. Device structure and experimental procedure

The development of Broadband multispectral PDs based on a-Si material is extremely difficult. This constraint is mainly due to the intrinsic limited absorption edge of this material. To overcome this absorption limitation, in this work we investigate a new multispectral PD

based on non-hydrogenated a-Si dwells on introducing intermediate Ti ultra-thin layers. In this context, Fig.1 (a) illustrates a cross-sectional view of the investigated a-Si/Ti multilayer-based PD device, where highly transparent ITO thin layer is deposited at the top of the structure to reduce the optical reflection losses [4]. The a-Si/Ti multilayer structure is sputtered considered on a glass substrate. As it is shown in this Figure, $d_{a-Si}=[d_{Si1},d_{Si2},...,d_{Sin}]$ *and* $t_{Ti}=[t_{Ti1},t_{Ti2},...,t_{Tij}]$ represent the thickness vector values associated with the silicon and titanium layers, respectively. Besides, n and j denote the number of a-Si and Ti sub-layers, respectively. The thickness of the PD device is $t_{a\text{-}Si/Ti}$. For the numerical simulation framework, the optical properties (absorbance, reflectance and transmittance) of the investigated PD structure are calculated using FDTD method provided SILVACO software [24].

As far as we are concerned, the development of highly efficient and low-cost multispectral sensors through intuiting the multi-layer structural, geometrical and electrical parameters by using the well-known optical and electrical properties of PDs is not sufficient to achieve the best electrical performances and highest photoresponsivity over a wide spectrum range. Alternatively, we believe that sophisticated numerical optimization strategies behaving like predictive simulations are required to forecast the sensor performance. In this context, the use metaheuristic optimization approaches such as GA technique is a powerful tool for identifying the optimal geometrical configuration of the a-Si/Ti multilayer structure to achieve the highest multispectral photoresponsivity. In this context, modeling and optimization frameworks based on FDTD and GA method are considered in the present work to predict the optical performances of the investigated a-Si/Ti structure. This technique is implemented to selecting the most suitable a-Si/Metal multilayer offering the highest absorbance efficiency over a wide spectrum range. The electrical transport model is not included in the performed predictive simulation. The introduction of the electrical modeling

combined with FDTD optical modeling in GA-based computation is time consuming due to the use of complex multilayer design with a high number of sub-layers. To do so, Fig.1 (b) shows the flowchart of the adopted hybrid design approach based on combined GA and numerical simulation techniques. The optical device properties are simulated using 2D-FDTD method. More details regarding the suggested modeling approach can be found in our previously published works [25-27].

The simulated spectral absorbance using FDTD technique is explored to formulate the objective (fitness) function, which will be minimized using GA-based optimization method. The fitness function is given by the following formula

$$Fitness\ (X_i) = \left(\frac{1}{A[\lambda_{\min}, \lambda_{\max}]} \right) \quad (1)$$

where A represents the average absorbance over the spectral range of $[\lambda_{\min}, \lambda_{\max}]$ with $\lambda_{\min} = 200nm$ and $\lambda_{\max} = 1100nm$ are respectively the minimum and the maximum wavelength values considered for broadband photosensing of PDs, X_i denotes the design parameter vector. Various metals (Ag, Au, Ni and Ti) are introduced in the optimization procedure. After carrying out the optimization procedure, the resulted design parameter vector of the investigated a-Si/Ti multilayer active-film is given by $X_i = (d_{a-Si} = [20nm, 36nm, 50nm, 40nm], t_{ITO} = 20nm, t_{Ti} = [9nm, 8nm, 7nm],\ j = 3)$. Fig.1 (c) shows the absorbance spectrum of the optimized a-Si/Ti structure. While the optimized metal is the Titanium, the optimized PD structure reveals a very high average absorbance of 81.3% over UV-Vis-NIR spectral range, indicating its broadband sensing properties. This makes it a promising candidate for elaborating highly efficient and low-cost multispectral photodetectors. This enhancement is attributed to the role of GA-based optimization tool in selecting the appropriate multilayer structure through promoting enhanced light-scattering

effects. The obtained design will be used to elaborate the optimized a-Si/Ti multilayer sensor, which is the main objective of the next part.

The proposed structure can be elaborated at deposition temperatures of 300 K, where the optimized a-Si/Ti multilayer is suggested on glass substrate. This is considered as a major advantage for the development of low-cost broadband photodetectors. In fact, the proposed structure can be prepared on Silicon substrate. However, the use of Silicon platform based on CMOS technology can impose the high thermal budget process and can also affect the device optical properties [28]. On the other hand, the use of back-end-of-line (BEOL) requires a complex structure involving contacts, insulating layers (dielectrics), metal levels, and bonding sites for chip-to-package connections. This can in turn affect the device optical behavior and the multispectral photodetection ability. Thus, these challenges should be taken into account for the realization of multispectral photodetectors compatible with the state-of the art CMOS technology. On the other hand, from an application perspective, it is important to note that the proposed a-Si/Ti multilayer can be developed on flexible substrates.

The elaboration of the optimized PD is based on three-step manufacturing processes. In the beginning, glass substrates were ultrasonically cleaned up using an ultrasonic bath and commercial detergent and then dried under a nitrogen jet procedure. Afterwards, successive deposition of the optimized a-Si and Ti thin-films on the glass substrate was carried out using *RF* magnetron sputtering technique (MOORFIELD MiniLab 060). To do so, p-type Si and Ti targets with high purity of 99.99% were used. This experimental technique is commonly used to elaborate high-quality thin-layers [29-31]. The sputtering process of a-Si and Ti sub-layers was performed in a pure *Ar* atmosphere with a pressure of 1.5 Pa. The deposition parameters were carefully tuned in order to obtain unhydrogenated a-Si state, Besides, the targets to substrate distances were kept at 6.5 cm and 5.1 cm for the Titanium and Si materials, respectively. The sputtering deposition parameters for all sub-layers are summarized in

Table.1. The ITO ultrathin film was deposited on the sputtered a-Si/Ti multilayer by using targets with 90 wt% In_2O_3 and 10 wt% SnO_2. The sputtering process for ITO thin-film was carried out in a mixture atmosphere of *Ar* and O_2 (*Ar: 66%, O_2: 33%*), where high-purity argon (99.99%) and oxygen (99.99%) gases are used. It is worthy to note that the RF sputter was calibrated before the deposition of deferent thin films, where each layer was separately grown on glass substrates to select the appropriate deposition parameters.

In order to assess the optoelectronic performances of the fabricated sensor, structural and optical characterizations were conducted using X-ray diffraction measurements (ARL Equinox 3000) for 2θ diffraction angle scans of [25°-80°] and UV-Visible-NIR spectrophotometer (F10-RT-UV). The morphological characteristics of the prepared sample were analyzed using scanning electron microscopy (SEM), where the surface (top) was imaged with a Zeiss Gemini SEM 500 with a field emission Schottky source. The semiconductor characterization system (Keithley 4200-SCS) was employed to measure the current-voltage characteristics of the prepared device under dark and illumination conditions.

3. Results and discussions

The aim of this work is to investigate the role of introducing a-Si/Ti multilayered structure with optimized geometry in improving the photosensing performances of PDs over a wide spectral range. The structural properties of the prepared sample based on embedded a-Si and *Ti* sputter-deposited thin-films are investigated using XRD technique. In this context, Fig.2 (a) shows XRD measurements for (2θ) diffraction angle scanning from 25° to 80° of the prepared samples based on ITO/a-Si thin-film and a-Si/Ti multilayered structure. The XRD pattern of the elaborated sample with ITO/a-Si shows a low-intensity XRD peak indexed to the (222) crystal plane of the ITO material. It can be also seen from this spectra the presence of a diffraction peak at 28.5° angle, corresponding the (111) facets of silicon. This indicates that the sputtering of thick Si films ($t_{a\text{-}Si}$=130 nm) enables the formation of Si microcrystals.

However, it can be noticed from the XRD pattern of the elaborated a-Si/Ti multilayer structure depicted in Fig.2 (a), the amorphous state of the silicon and ITO sputtered layers, where no coherent XRD peaks are matching these materials. The obtained crystalline characteristics can be explained by the ultralow thickness of the deposited silicon sub-layers, which can prevent reaching the crystallization phase of the Si material. On the other hand, this pattern demonstrates the presence of crystallized Ti metal, manifesting (101)-oriented film at the diffraction angle of 39.5°. This highlights the beginning of the crystallization phase of the deposited Ti inter-layers. Fig.2 (b) shows the SEM top surface image of the fabricated ITO/a-Si/Ti multilayered sample. It can be seen from this micrograph that granulated ITO surface with roughness characteristics is observed. This indicates that the growth is essentially columnar for the embedded a-Si and Ti sub-layers, which further explains the obtained amorphous state of the sputtered silicon thin-films as it is shown in Fig.2 (a). In other words, as the a-Si and Ti thin-films are embedded by RF sputtering technique, the structure roughness significantly increases and when the grain size is superior to the film thickness, the growth becomes columnar particularly for the deposited layers closest to the surface.

One of the most important criteria that active layers of multispectral PDs should satisfy is to offer a broadband absorption property. To assess the absorption capabilities of the prepared sample based on stacked a-Si and Ti sub-layers with optimized geometry, the absorbance spectra of the elaborated samples were extracted and illustrated in Fig.3. It can be observed from this figure that significant changes concerning the optical behavior of the PD active film are achieved by inserting an optimized a-Si/Ti multilayer. It demonstrates highly improved absorption efficiency exceeding 85% over UV-Vis-NIR spectral range as compared to that of a-Si thin-film (28.2%). This yields a high relative enhancement of 183%. This achievement is due to the effectiveness of the introduced FDTD-GA hybrid approach in promoting enhanced light trapping capabilities of embedded a-Si and Ti sub-layers with suitable geometry. In other

words, the introduction of Ti intermediate metal films within the a-Si layer can generate optical micro-cavities, which leads to extend the optical path in the PD active layer thereby resulting in a broadband absorption characteristic. On the other hand, it can be observed from Fig.3 that the obtained experimental results are found in a good agreement with the theoretical ones, where only small discrepancies between both experimental and numerical data are observed over the UV spectral range. This can be attributed to the experimental condition, the prepared structure shows surface roughness and the growth is columnar particularly for the top sub-layers as it is shown in Fig.2. This unexpected effect has also contributed to further enhancing the multilayer light trapping capability due to the development of nanostructured columnar for the sputtered sub-layers closest to the surface. In this context, effects related to experimental conditions such as the resulted columnar structure are not included in the performed simulations. This explains the above-mentioned discrepancies concerning the obtained absorbance spectra from simulation and experimental data. To achieve a close resemblance between the numerical and experimental data, several experimental parameters of the sputtering technique should be taken into account, which is considered extremely difficult. Therefore, the fabrication of such an optimized a-Si/Ti multilayered structure as an MSM photodetector can extend the light harvesting capability into the visible and NIR spectral ranges, making it very promising candidate for the development of high-responsivity broadband PDs at low-cost.

To further investigate the multispectral photoresponse of the prepared PD based on stacked a-Si and Ti thin-films, the sample is realized as an MSM photodetector. In this framework, top and bottom gold contacts were evaporated via E-beam evaporation technique as it is shown in Fig.1 (a). The fabricated device was then illuminated by monochromatic light signals with wavelength values of 365 nm, 550 nm and 900 nm using LED lamps. Moreover, to show the capability of the proposed experiment assisted by FDTD-GA hybrid approach in

developing broadband PDs based on simple and low-cost structures, the device sensitivity and responsivity are estimated using the following formulas

$$S = \frac{I_{ph} - I_{dark}}{I_{dark}} \times 100 \quad (1)$$

$$R = \frac{I_{ph}}{P_i} \text{ [A/W]} \quad (2)$$

where I_{ph} and I_{dark} represent the measured currents under illumination and dark conditions, P_i denotes the optical power density.

The measured I-V characteristics in darkness and under illumination conditions of the prepared sensors based on a-Si and a-Si/Ti multilayer active films are depicted in Fig.4 (a) and (b) respectively. It can be seen from Fig.4 (a) that the a-Si based PD shows a good photoresponse only in the UV range. On the other hand, Fig.4 (b) demonstrates the ability of the prepared PD with embedded a-Si and Ti sub-layers for providing multispectral photodetection capability. The device shows excellent sensing properties with high photocurrent values of 0.68 mA, 0.22 mA and 0.1 mA under UV, visible and NIR lights, respectively at an applied voltage of 3V. Moreover, the elaborated photodetector shows high sensitivity values of 1128, 681 and 380 over UV, Visible and NIR spectral bands. Such finding correlates well with the above-outlined broadband absorption characteristic of the optimized structure based on embedded a-Si and Ti thin-films. Basically, the latter structure shows an extended absorption to the visible and NIR regions, which can enables enhancing the carrier generation mechanism. This effect leads to achieve an improved broadband photoresponse. More importantly, the use of stacked a-Si and Ti layers can enlarge the depletion layer in the active layer due to the Schottky nature of the a-Si/Ti contact. This can in turn improve the separation mechanism of the photo-excited e/h pairs, thus reducing recombination losses. The self-powered property, which describes the ability of device to operate without the need of any applied voltage (V_{input}=0V) is highly required for developing

high-performance and low-power consumption photodetectors. It seems important to assess the ability of the prepared photodetector to offer the self-powered characteristic. In this context, it can be observed from Fig.4 (b) that the proposed PD based on a-Si/Ti multilayer provides a favorable photocurrent at zero bias condition, where the measured I-V curves are shifted to negative voltages. This phenomenon is attributed to the degraded homogeneity of the deposited sub-layers, where the sputtering of a-Si and Ti layers closest to the surface is principally columnar as it is above-outlined. In other words, this effect can affect the homogeneity of both contacts, which leads to an asymmetrical electrical behavior as it is shown in Fig.4 (b).

On the other hand, Fig.4 (a) and (b) show that the prepared a-Si/Ti multilayer device exhibits a high current as compared to that of the conventional device in darkness. This is mainly due to the improved conductivity of the device, where introducing Ti metal layer induces significant changes in the device resistive behavior. This can lead to reduce the device series resistance and increase the dark current. To consolidate this explanation, the series resistance values of the prepared devices based on a-Si/Ti multilayer and a-Si thin-film are extracted using the electrical characterization methodology provided in our previous work [31]. The results show that the elaborated a-Si/Ti multilayer structure exhibits lower series resistance of 8×10^3 Ω as compared to that of the conventional a-Si-based device (2×10^4 Ω).

Fig.5 depicts the measured spectral responsivity of the elaborated samples based on a-Si thin-film and stacked a-Si and Ti layers. Clearly, the proposed sensor demonstrates a high responsivity over a large spectral band from UV to NIR as compared to the conventional device. The prepared PD with a-Si/Ti multilayered active film exhibits superior responsivity values of 1.9 A/W, 1.24 A/W and 93 mA/W under UV, visible and NIR illumination conditions, respectively. The enhanced multispectral photoresponse characteristics are mainly attributed to the role of the optimized a-Si/Ti multilayer in achieving the dual benefits of

enhanced photogenration and collection mechanisms. In other words, the introduced FDTD-GA hybrid approach enables selecting the optimized a-Si/Ti multilayer structure offering the highest and broadband absorption. This leads to enhance the quantity of photo-induced carriers and thereby the device responsivity. On the other hand, a-Si/Ti electronic interface exhibits a Schottky behavior leading to induce localized depletion regions. This would reduce the recombination effects thus enhancing the device collection efficiency. Therefore, the combination of these benefits has allowed developing high-performance multispectral photodetector based on cost-effective structure, which can be prepared in room temperature conditions.

To show the strength of the prepared multispectral PD based on a simple and low-cost embedded a-Si and Ti thin-films as compared to recently developed ones, a comparative performance analysis is carried out. Accordingly, the associated FoM parameters including current ratio (I_{ON}/I_{OFF} ratio), responsivity and detectivity are extracted and summarized in Table.2. This table confirms the ability of the optimized structure for outperforming other perovskite, silicon and nanostructured multispectral PD structures in terms of FoM parameters [32-41]. Although some reported devices demonstrated superior visible photoresponse, they either exhibited a compromised UV sensitivity, stability issues and/or required the use of critical raw materials and processing complexity. Alternatively, the present PD with stacked a-Si and Ti thin-films provides a new strategy for achieving high and broadband photosensing characteristics at low manufacturing cost. These results clearly demonstrate the great potential of the proposed a-Si/Ti multilayer structure for multispectral photodetection application.

4. Conclusion

In this work, we have developed a new high-photoresponsivity multispectral PD based on ITO/a-Si multilayer structure. The numerical simulation and optimization of the structure using combined FDTD-GA approach offer improved photoresponsivity and broadband absorption

capabilities. The optimized design was employed in fabricating multispectral photodetector using RF magnetron sputtering technique. The device structural and optical properties were investigated using XRD and UV-Vis-NIR spectroscopy methods. It was found that excellent UV-Vis-NIR absorbance with over than 80% average value was recorded which can lead to improve the device photoresponsivity. In this context, the elaborated sensor offers ultra-high responsivity values of 1.9 A/W, 1.24A/W and 0.93 A/W under UV, visible and NIR illumination, respectively. This multispectral photodetection property is mainly attributed to the effective light-management provided by the optimized design. Moreover, it is demonstrated that the elaborated PD based on embedded a-Si and Ti sub-layers can operate in self-powered mode, showing a favorable photocurrent of 0.4 µA. The proposed elaboration methodology can contribute in a fascinating breakthrough towards broadband multispectral photodetector devices based on Si-photonics platform.

References

[1] D. A. B. Miller, "Optical interconnects to silicon," IEEE J. Sel. Top. Quantum Electron., vol. 6, pp. 1312-1317, 2000.

[2] C. Sun, et al "Single-chip microprocessor that communicates directly using light," Nature, vol. 528, pp. 534-538, 2015.

[3] S. Manipatruni, M. Lipson, and I. A. Young, "Device Scaling Considerations for Nanophotonic CMOS Global Interconnects," IEEE J. Sel. Top. Quantum Electron., vol. 19, pp. 1077-1086 , 2013.

[4] H. Ferhati, F. Djeffal, N. Boubiche, A. Benhaya, J. Faerber, F. Le Normand, N. Javahiraly and T. Fix, "Absorption enhancement in amorphous Si by introducing RF sputtered Ti intermediate layers for photovoltaic applications," Materials Science and Engineering: B, vol.269, pp. 115152, 2021.

[5] W. Ouyang, F. Teng, J.-H. He, X. Fang, "Enhancing the Photoelectric Performance of Photodetectors Based on Metal Oxide Semiconductors by Charge-Carrier Engineering," Adv. Funct. Mater., vol. 29, pp.1807672, 2019.

[6] H. Ferhati, F. Djeffal, "Planar junctionless phototransistor: A potential high-performance and low-cost device for optical-communications," Optics & Laser Technology, vol. 97, pp.29-35, 2017.

[7] M. Zhang, D. Zhang, and F. Jing, "Hybrid Photodetector Based on ZnO Nanofiber Polymers with High Spectrum Selectivity," IEEE Photon. Technol. Lett., vol. 28, pp. 1677-1679, 2016.

[8] N. Naderi, M. Moghaddam, "Ultra-sensitive UV sensors based on porous silicon carbide thin films on silicon substrate," Ceramics International., Vol. 46, pp. 13821-138260, 2020.

[9] C. Li, W. Huang, L. Gao, H. Wang, L. Hu, T. Chen and H. Zhang, "Recent advances in solution-processed photodetectors based on inorganic and hybrid photo-active materials," Nanoscale, vol.12, pp. 2201-2227, 2020.

[10] K. Benyahia, F. Djeffal, H. Ferhati, A. Bendjerad, A. Benhaya, A. Saidi," Self-powered photodetector with improved and broadband multispectral photoresponsivity based on ZnO-ZnS composite," J. Alloy. Compd., vol. 859, pp.158242, 2021.

[11] H. S. Nalwa, "A review of molybdenum disulfide (MoS_2) based photodetectors: from ultra-broadband, self-powered to flexible devices," RSC Adv., vol.10, pp. 30529, 2020.

[12] C. Ji, X. Huang, D. Wu, Y. Tian, J. Guo, Z. Zhao, Z. Shi, Y. Tian, J. Jie, and X. Li, "Ultrasensitive self-driven broadband photodetector based on 2D-WS_2/GaAs type-II Zener heterojunction," Nanoscale, vol.12, pp. 4435-4444, 2020.

[13] J. Miao and F. Zhang, "Recent progress on highly sensitive perovskite photodetectors," J. Mater. Chem. C, vol.7, pp. 1741-1791, 2019.

[14] J. Huang, J. Jiang, L. Hu, Y. Zeng, S. Ruan, Z. Ye and Y-J. Zeng, "Self-powered ultraviolet photodetector based on CuGaO/ZnSO heterojunction," J. Mater. Sci.: Mater. Electron., vol.55, pp. 9003-9013, 2020.

[15] X. Xu, J. Chen, S. Cai, Z. Long, Y. Zhang, L. Su, S. He, C. Tang, P. Liu, H. Peng and X. Fang, "A Real-Time Wearable UV-Radiation Monitor based on a High-Performance p-CuZnS/n-TiO_2 Photodetector", Adv. Mater., vol. 25, pp. 1803165, 2018.

[16] M. Patel, P. M. Pataniya, V. Patel, C. K. Sumesh and D. J. Late, "Large area, broadband and highly sensitive photodetector based on ZnO-WS_2/Si heterojunction," Solar energy, vol.206, pp. 974-982, 2020.

[17] H. Ferhati and F. Djeffal, "High-Responsivity MSM Solar-Blind UV Photodetector Based on Annealed ITO/Ag/ITO Structure Using RF Sputtering," IEEE Sens. J., vol. 19, pp. 7942 - 7949, 2019.

[18] S. Bhandari, D. Mondal, S. K. Nataraj and R. G. Balakrishna, "Biomolecule-derived quantum dots for sustainable optoelectronics," Nanoscale Adv., vol.1, 913-936, 2018.

[19] S. Li, Y. Zhang, W. Yang, H. Liuand and X. Fang, "2D Perovskite $Sr_2Nb_3O_{10}$ for High-Performance UV Photodetectors," Adv. Mater., vol.32, pp. 1905443, 2020.

[20] T. T. Nguyen, M. Patel and J. Kim, "Self-powered transparent photodetectors for broadband applications," J. Surf. Interfac., vol.23, pp. 100934, 2021.

[21] B. Wang, Shi P. Zhong, Z. B. Zhang, Z. Q. Zheng, Y. P. Zhang and H. Zhang, "Broadband photodetectors based on 2D group IVA metal chalcogenides semiconductors," Appl. Mater. Today, vol.15, pp. 115-138, 2019.

[22] C-H. Liu, Y-C. Chang, T. B. Norris and Z. Zhong, "Graphene photodetectors with ultra-broadband and high responsivity at room temperature," Nat. Nanotechnol., vol. 9, pp. 273–278, 2014.

[23] J. Yao and G. Yang, "2D material broadband photodetectors," Nanoscale, vol. 12, pp. 454-476, 2020.

[24] Atlas User's manual, SILVACO TCAD, 2012.

[25] F. Srairi, F. Djeffal and H. Ferhati,“ Efficiency increase of hybrid organic/inorganic solar cells with optimized interface grating morphology for improved light trapping,” Optik, vol. 130, pp. 1092-1098, 2017.

[26] F. Djeffal, T. Bendib, R. Benzid, A. Benhaya, “An approach based on particle swarm computation to study the nanoscale DG MOSFET-based circuits,” Turk. J. Elec. Eng & Comp Sci., vol. 18, pp. 1131-1140, 2010.

[27] F. Djeffal, H. Ferhati, “A new high-performance phototransistor design based on both surface texturization and graded gate doping engineering,” J. Comput. Electron, vol. 15, pp. 301–310, 2016.

[28] H. Ferhati, F. Djeffal, D.Arar and Z.Dibi, “Role of metal layer in improving the UV-photodetector performance of TiO2/Metal/TiO2/Si structure,” Journal of Luminescence, vol.191, pp. 117-121, 2017.

[29] E. Márquez, E. Saugar, J. M. Díaz, C. García-Vázquez, S. M. Fernández-Ruano, E. Blanco, J. J. Ruiz-Pérez and D. A. Minkov, “The influence of Ar pressure on the structure and optical properties of nonhydrogenated a-Si thin films grown by rf magnetron sputtering onto room temperature glass substrates”, J. Non-Cryst Solids, vol. 517, pp. 32-43, 2019.

[30] S. Y. Lee, Y. S. Park, T. Seong, “Optimized ITO/Ag/ITO multilayers as a current spreading layer to enhance the light output of ultraviolet light-emitting diodes,” J. Alloy. Compd., vol.776, pp. 960-964, 2019.

[31] A. Benhaya, F. Djeffal, K. Kacha, H. Ferhati, A. Bendjerad, “Role of ITO ultra-thin layer in improving electrical performance and thermal reliability of Au/ITO/Si/Au structure: An experimental investigation,” Superlattices Microstruct., vol.120, pp. 419-426, 2018.

[32] H. Ahmad, N. Afzal, M. Rafique, A. A. Ahmed, R. Ahmad and Z. Khaliq, “Post-deposition annealed MoO_3 film based high performance MSM UV photodetector fabricated on Si(100),” Ceramics International, vol. 47, pp. 20477-20487, 2020.

[33] D. Wu, J. Guo, J. Du, C. Xia, L. Zeng, Y. Tian, Z. Shi, Y. Tian, K. J. Li, Y. H. Tsang and J. Jie, “Highly Polarization-Sensitive, Broadband, Self-Powered Photodetector Based on Graphene/$PdSe_2$/Germanium Heterojunction,” ACS Nano, vol. 13, pp. 9907−9917, 2019.

[34] Y. Zhang, W. Xu, X. Xu, J. Cai, W. Yang, and X. Fang, “Self-Powered Dual-Color UV–Green Photodetectors Based on SnO_2 Millimeter Wire and Microwires/$CsPbBr_3$ Particle Heterojunctions”, J. Phys. Chem. Lett., vol. 10, pp. 836–841, 2019.

[35] C. L. Hsu, H. Y. Wu, C. C. Fang, and S. P. Chang, "Solution-Processed UV and Visible Photodetectors Based on Y-Doped ZnO Nanowires with TiO_2 Nanosheets and Au Nanoparticles," ACS Appl. Mater. Interfaces, vol.5, pp. 2087-2095, 2018.

[36] M. Das, S. Sarmah, D. Barman, B. K. Sarma and D. Sarkar, "Distinct band UV–Visible photo sensing property of ZnO-Porous silicon (PS): p-Si hybrid MSM heterostructure," Mater. Sci. Semicond. Process., vol.118, pp. 105188, 2020.

[37] F. Cao, W. Tian, K. Deng, M. Wang and L. Li, "Self-Powered UV–Vis–NIR Photodetector Based on Conjugated-Polymer/$CsPbBr_3$ Nanowire Array," Adv. Funct. Mater., vol.29, pp. 1906756, 2019.

[38] H. Ferhati, F. Djeffal and N. Martin, "Highly improved responsivity of self-powered UV–Visible photodetector based on TiO_2/Ag/TiO_2 multilayer deposited by GLAD technique: Effects of oriented columns and nano-sculptured surface," Appl. Surf. Sci., vol.529, pp. 147069, 2020.

[39] M. S. Mahdi, K. Ibrahim, N. M. Ahmed, A. Hmood, F. I. Mustafa, S. A. Azzez and M. Bououdina, "High performance and low-cost UV–Visible–NIR photodetector based on tin sulphide nanostructures," J. Alloy. Compd., 735, 2256-2262, 2018.

[40] Z. Zheng, L. Gan, J. Zhang, F. Zhuge and T. Zhai, "An enhanced UV–Vis–NIR and flexible photodetector based on electrospun ZnO nanowire array/PbS quantum dots film heterostructure," Adv. Sci., vol.4, pp.1600316, 2017.

[41] G. Chatzigiannakis, A. Jaros, R. Leturcq, J. Jungclaus, T. Voss, S. Gardelis and M. Kandyla, "Laser-Microstructured ZnO/p-Si Photodetector with Enhanced and Broadband Responsivity across the Ultraviolet–Visible–Near-Infrared Range," ACS Appl. Electron. Mater., vol.9, pp. 2819–2828, 2020.

Figures caption:

Fig.1 (a): Device structure with MSM Schottky PD configuration based on the proposed a-Si/ Ti multilayer structure. **(b)** Flowchart of the adopted hybrid design approach based on combined GA and numerical simulation techniques. **(c)** Absorbance spectrum of the optimized a-Si/Ti multilayered structure.

Fig.2 (a) X-ray diffraction patterns of the elaborated a-Si/Ti structure with $t_{a\text{-}Si/Ti}$=170nm and t_{ITO}=20nm. **(b)** SEM images of top surface of the elaborated a-Si/Ti multilayer structure using RF magnetron sputtering technique.

Fig.3: Absorbance spectra of the prepared ITO/a-Si and a-Si/Ti multilayer samples with $t_{a\text{-}Si/Ti}$ =170nm and t_{ITO}=20nm.

Fig.4: Measured I-V characteristics under dark and light-exposure conditions in UV, visible and NIR spectrum bands of **(a)** the conventional device with a-Si active layer, **(b)** the prepared PD based on embedded a-Si and Ti sub-layers.

Fig.5: Spectral photoresponsivity of the prepared PD structures based on a-Si thin-film and a-Si/Ti multilayer.

Tables:

Table.1: Deposition parameters of the sputtered ITO/a-Si/Ti multilayer structure.

Table.2: Overall performance comparison between the elaborated PD and several reported multispectral photodetector devices.

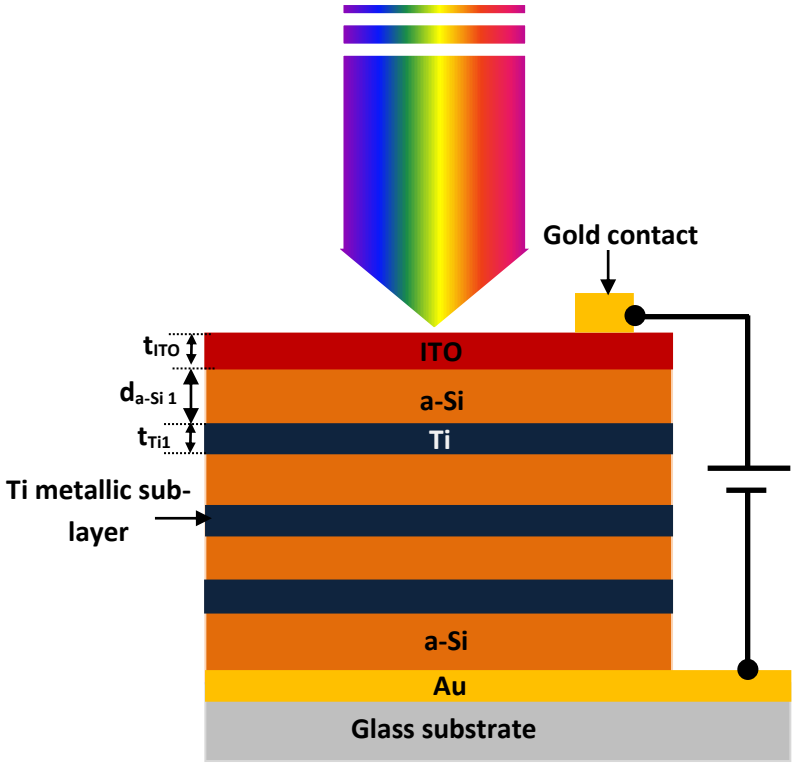
Gold contact
t_{ITO}
ITO
$d_{a\text{-}Si\ 1}$
a-Si
t_{Ti1}
Ti
Ti metallic sub-layer
a-Si
Au
Glass substrate

(a)

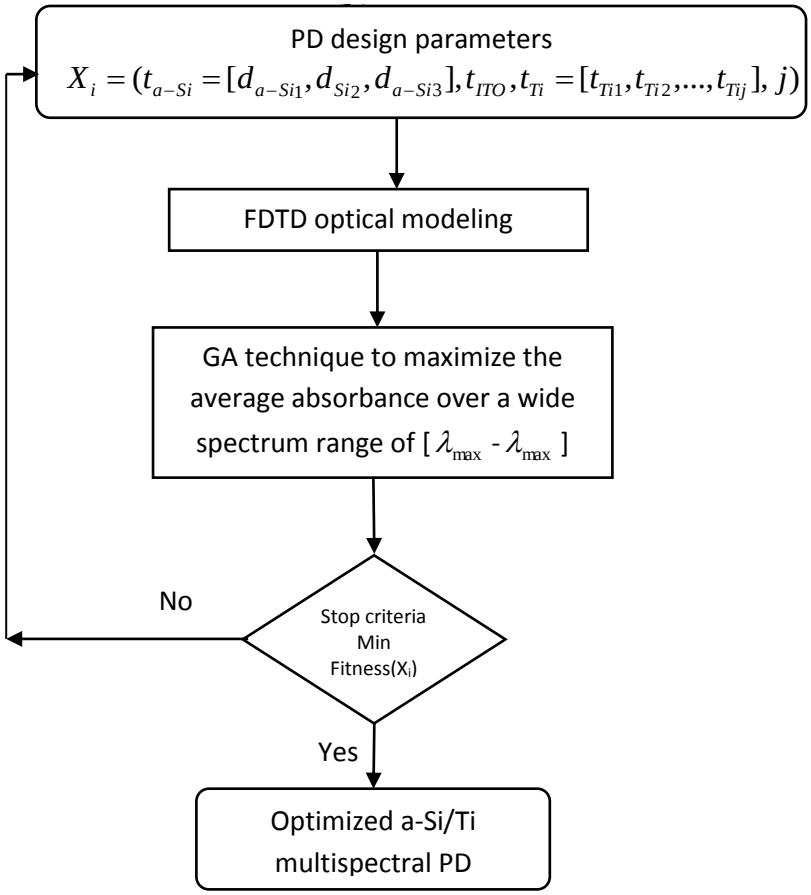
PD design parameters
$X_i = (t_{a-Si} = [d_{a-Si1}, d_{Si2}, d_{a-Si3}], t_{ITO}, t_{Ti} = [t_{Ti1}, t_{Ti2}, ..., t_{Tij}], j)$
FDTD optical modeling
GA technique to maximize the average absorbance over a wide spectrum range of [λ_{max} - λ_{max}]
Stop criteria Min Fitness(X_i)
No
Yes
Optimized a-Si/Ti multispectral PD

(b)

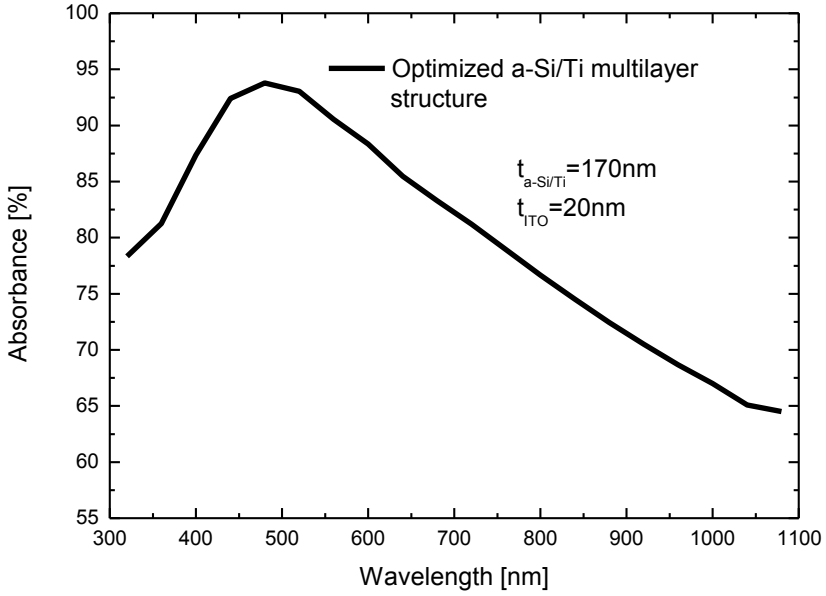
Optimized a-Si/Ti multilayer structure
$t_{a\text{-}Si/Ti}$=170nm
t_{ITO}=20nm
Absorbance [%]
Wavelength [nm]
100
95
90
85
80
75
70
65
60
55
300
400
500
600
700
800
900
1000
1100

(c)

Figure.1

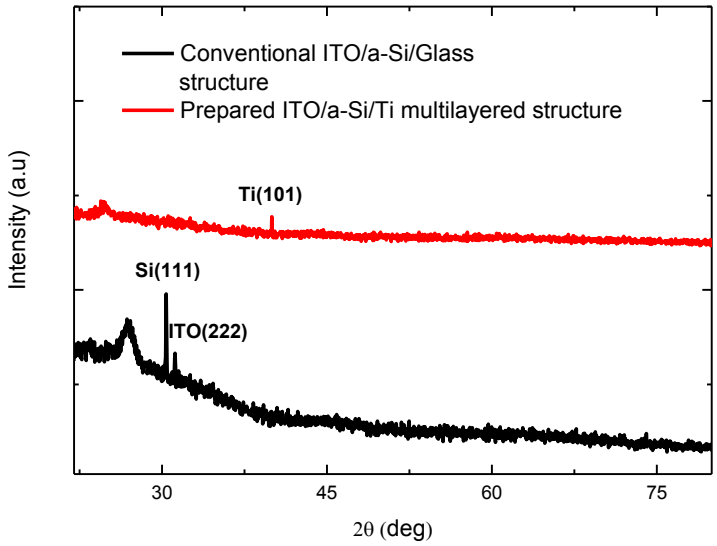
Conventional ITO/a-Si/Glass structure
Prepared ITO/a-Si/Ti multilayered structure
Ti(101)
Si(111)
ITO(222)
Intensity (a.u)
30
45
60
75
2θ (deg)

(a)

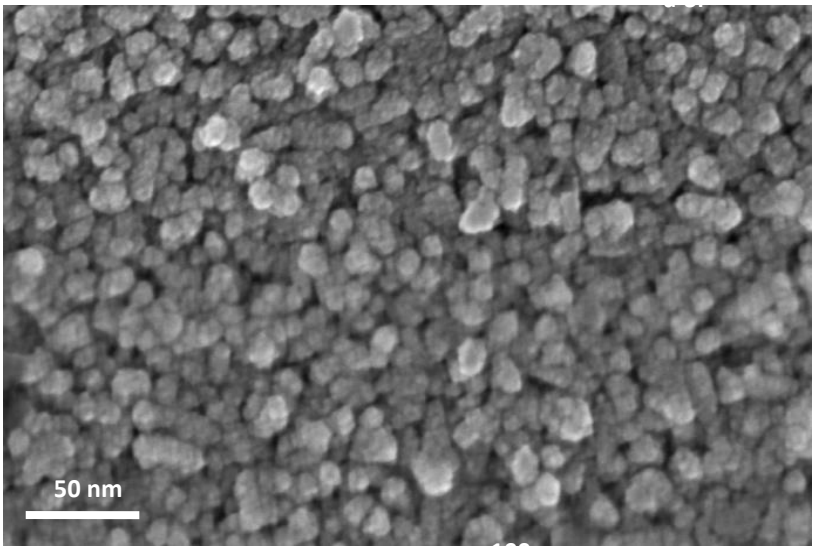
50 nm

(b)

Figure.2

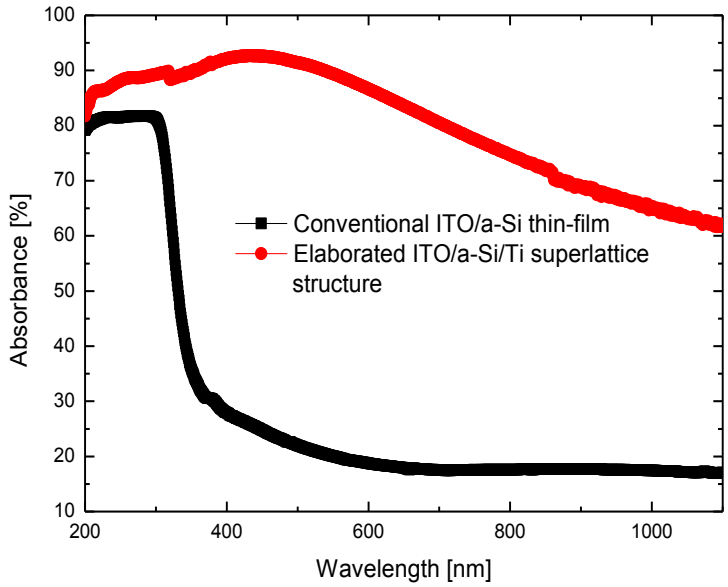
Absorbance [%]
Wavelength [nm]
Conventional ITO/a-Si thin-film
Elaborated ITO/a-Si/Ti superlattice structure
100
90
80
70
60
50
40
30
20
10
200
400
600
800
1000

Figure.3

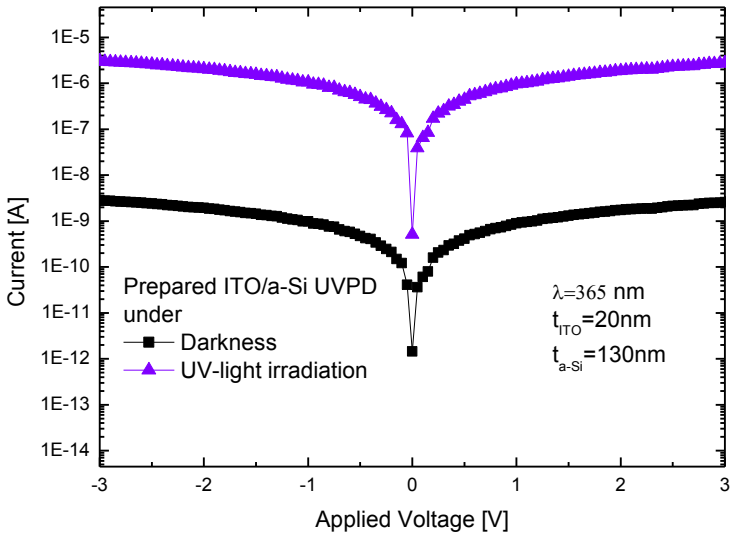
Current [A]
1E-5
1E-6
1E-7
1E-8
1E-9
1E-10
1E-11
1E-12
1E-13
1E-14
-3
-2
-1
0
1
2
3
Applied Voltage [V]
Prepared ITO/a-Si UVPD
under
Darkness
UV-light irradiation
λ=365 nm
t_ITO=20nm
t_a-Si=130nm

(a)

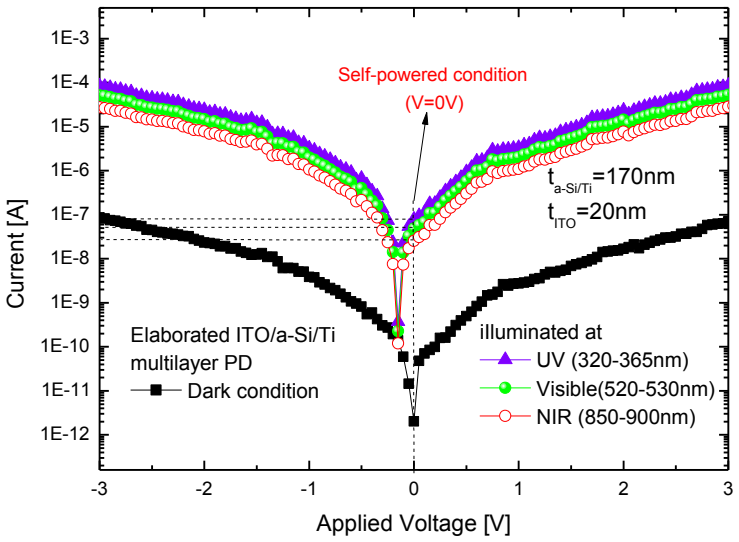
Current [A]
1E-3
1E-4
1E-5
1E-6
1E-7
1E-8
1E-9
1E-10
1E-11
1E-12
-3
-2
-1
0
1
2
3
Applied Voltage [V]
Self-powered condition
(V=0V)
t_a-Si/Ti=170nm
t_ITO=20nm
Elaborated ITO/a-Si/Ti
multilayer PD
Dark condition
illuminated at
UV (320-365nm)
Visible(520-530nm)
NIR (850-900nm)

(b)

Figure.4

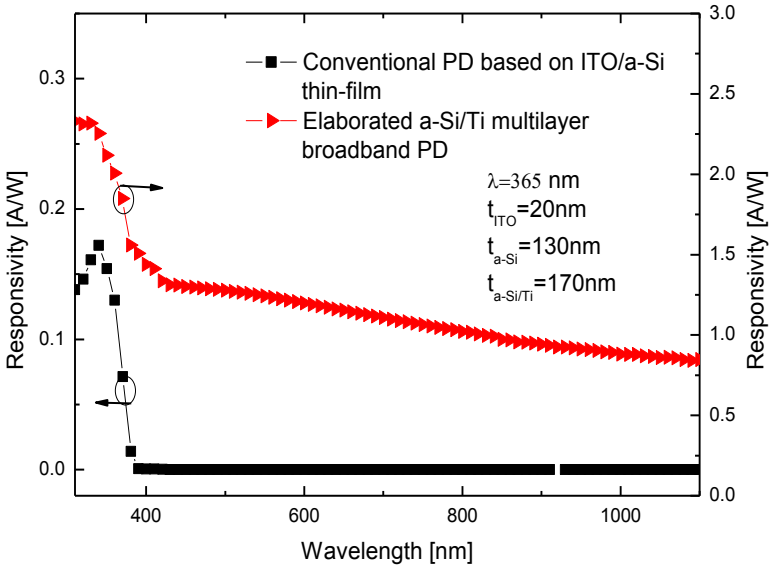
Conventional PD based on ITO/a-Si thin-film
Elaborated a-Si/Ti multilayer broadband PD
λ=365 nm
t_ITO=20nm
t_a-Si=130nm
t_a-Si/Ti=170nm
Responsivity [A/W]
Responsivity [A/W]
Wavelength [nm]
0.0
0.1
0.2
0.3
0.5
1.0
1.5
2.0
2.5
3.0
400
600
800
1000

Figure.5

Table.1

Parameter	**ITO**	**a-Si**	**Ti**
Target	(90% In_2O_3,10% SnO_2)	99.99% p-Si	99.99% Ti
Target to substrate distance (cm)	5	5.1	6.5
Gas composition (Ar: O_2)	(66%: 33%)	/	/
Substrate temperature (K)	300	300	300
power of *RF* source (W)	240	250	250
Working pressure (Pa)	1.5	1.5	1.5
deposition rate (nm/s)	0.2	0.4	0.7

Table.2

UV-Vis-NIR PD structures	UV (320-365 nm)			Visible (green) (515-525 nm)			NIR (880-900 nm)			Ref.
	I_{ON}/I_{OFF} (dB)	R (A/W)	D^* (Jones)	I_{ON}/I_{OFF} (dB)	R (A/W)	D^* (Jones)	I_{ON}/I_{OFF} (dB)	R (A/W)	D^* (Jones)	
MoO_3/c-Si heterojunction	63.2	0.41	3.9×10^{11}	-	-	-	-	-	-	[32]
Graphene/$PdSe_2$/Ge Heterojunction	20	0.69	1.2×10^{13}	28	1.72	2×10^{13}	55.9	4.7	7.4×10^{13}	[33]
SnO_2Microwire/$CsPbBr_3$ structure	35	0.03	1.6×10^{10}	35.5	0.46	1.2×10^{10}	-	-	-	[34]
Au NPs/p-ZnO NSs/n-ZnO	61.3	0.73	3.4×10^{12}	19.7	0.08	5.3×10^{11}	-	-	-	[35]
ZnO/Si heterjunction	66.2	0.55	4.8×10^{13}	-	0.68	5.8×10^{13}	-	-	-	[36]
Grating $CsPbBr_3/SnO_2$	61.8	0.22	1.2×10^{13}	52.4	0.01	4×10^{12}	53.1	0.086	2×10^{12}	[37]
Inclined TiO_2/Ag/ TiO_2 multilayer	137.2	0.2	5.3×10^{13}	107.6	0.12	3.5×10^{12}	-	-	-	[38]
SnS nanostructure	18	0.38	-	16.8	0.49	-	13.8	0.62	-	[39]
ZnO NWs/PbS QDs	59	0.51	3.4×10^{8}	39	0.07	4.9×10^{7}	26.8	0.11	4.2×10^{7}	[40]
Microstructured ZnO/Si	-	0.6	1×10^{10}	-	0.14	-	-	0.06	-	[41]
a-Si based PD	60.6	0.13	4×10^{12}	/	/	/	/	/	/	This work
Optimized a-Si/Ti structure	69.1	1.92	9.6×10^{12}	67.2	1.24	6.2×10^{12}	58.5	0.93	4.7×10^{12}	This work